COMPARISON BETWEEN VAPOR CHAMBER AND CONDUCTING FIN BRAYTON RADIATORS*

John W. Larson
General Electric Company
Missile and Space Division
King of Prussia, Pennsylvania

James P. Couch
National Aeronautics and Space Administration
Lewis Research Center
Cleveland, Ohio

ABSTRACT

Preliminary designs of both vapor chamber and conduction fin radiators were generated for a Brayton cycle space powerplant. Heat rejected by this radiator was about 15 KW. The designs are comparable in both size and weight for this Brayton application. Suitable working fluids for aluminum vapor chambers operating at 0° to 350°F include ammonia, benzene, pentane, and water (with liner).

INTRODUCTION

The Brayton cycle space powerplant, under development at the Lewis Research Center, uses an indirect heat rejection process with a heat rejection of about 15 KW. A compact heat exchanger transfers waste heat from the power conversion loop to a liquid coolant. This coolant is then circulated through a radiator where the waste heat is rejected to space. This radiator is called the primary radiator. In addition, an auxiliary circuit and radiator reject heat lost by cooling the powerplant electrical and other components. This radiator is called the secondary radiator.

At present, the configuration visualized for these radiators is an array of tubes through which coolant flows and to which are attached solid, conducting fins. It was anticipated that a significant reduction in radiator weight and area might be achieved by using "vapor chamber" fins. Therefore, preliminary designs for both radiator configurations have been generated and compared. The design specifications used in the comparison are shown in Figure 1.

VAPOR CHAMBER WORKING FLUIDS

A vapor chamber fin, or heat pipe, is a sealed duct containing a two-phase (vapor and liquid) working fluid. When heat is added to one portion of the vapor chamber, the working fluid evaporates. The vapor flows to a cooler portion where it condenses. The condensate is then returned to the heated portion by capillary action in a wick material which lines the inside of the vapor chamber (see Figure 2). By this mechanism a vapor chamber can exhibit a high effective thermal conductivity[1].

A high effective thermal conductivity means the temperature drop across the vapor chamber is small. This temperature drop is important in the design of a radiator. The smaller the temperature drop, the closer the radiator surface temperature is to the coolant temperature. In the limit, when the temperature drop is zero, the radiator would have its minimum or "ideal" area.

The temperature drop across the vapor chamber is the sum of the temperature drops from the coolant to the chamber wall, across the wall, across the evaporating layer, across the flowing vapor, across the condensing film, and across the chamber wall to the radiating surface. Of these, the temperature drops across the evaporating layer, the flowing vapor and the condensing film depend upon the choice of vapor chamber working fluid. For the vapor chamber designs considered, the pressure drop in the flowing vapor was very small. Thus, the temperature drop across the vapor was negligible (less than 0.1°F). The evaporative and condensing temperature drops vary significantly with working fluid. They can therefore be used to evaluate vapor chamber working fluids.

The evaporative and condensing temperature drops were estimated by assuming a physical model for the vapor chamber radiator. This model assumed a heat addition area and a heat rejection area. Knowing the operating temperature, the background temperature, and assuming an emissivity for the vapor chamber fin, the

*Sponsored by NASA, Lewis Research Center, under Contract NAS 3-10615.

[1] Grover, G. M., Cotter, T. P. and Erickson, G. F., "J. Applied Phys.," Vol 35, pp 1990, 1964

THERMAL HEAT REJECTION-	12.39 KWT PRIMARY, 2.19 KWT SECONDARY
RADIATOR COOLANT INLET TEMPERATURE -	288°F PRIMARY, 118°F SECONDARY
RADIATOR COOLANT OUTLET TEMPERATURE-	64° F PRIMARY AND SECONDARY
EFFECTIVE RADIATOR SINK TEMPERATURE -	-10° F
RADIATOR SURFACE THERMAL EMISSIVITY-	0.85
RADIATOR COOLANT	DOW CORNING 200, 2 CENTISTOKES AT 77° F
PRIMARY PRESSURE DROP -	25 PSI MAXIMUM
RELIABILITY-	0.99 OR 0.999 FOR 5 YEARS
SUPPORTED LOAD -	5000 LB
STRUCTURAL MATERIAL -	ALUMINUM 6061 -T6

Figure 1. Design Specifications for the Brayton Cycle Radiator

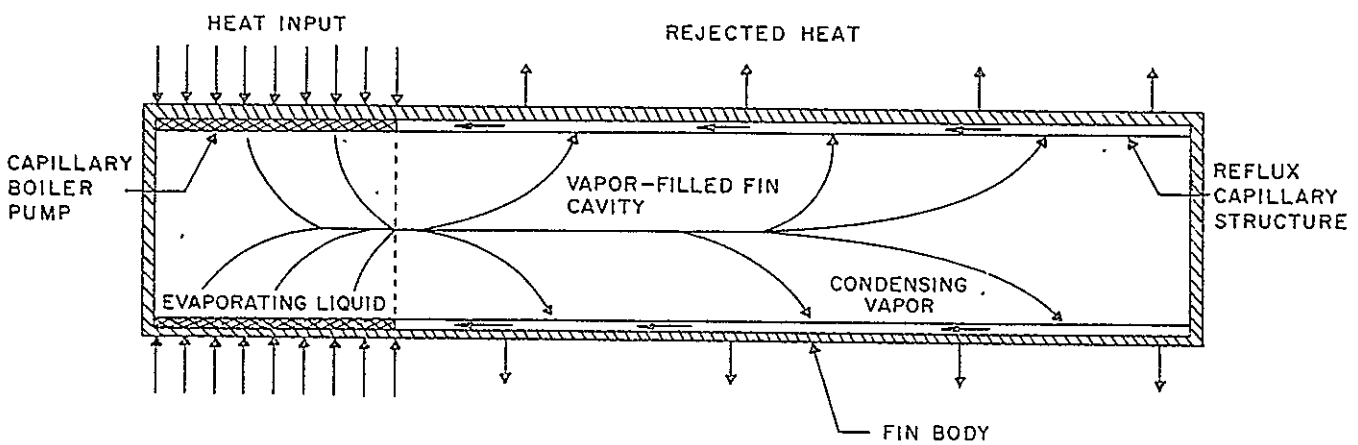

Figure 2. Vapor Chamber Fin Concept

heat load of the vapor chamber was calculated. The evaporative and condensing heat fluxes were then determined. The evaporative temperature drop was calculated by the method described in McAdams[2] using the peak heat flux correlation of Cichelli and Bonilla[3]. The Cichelli and Bonilla correlation is based on pool boiling data for several organic fluids. It is felt this correlation provides a reasonable standard for evaluation of working fluids until actual experimental studies are completed later in this program. The condensing temperature drop was calculated assuming only conduction across a 0.010 inch film of the working fluid. Figures 3 and 4 show evaporative and condensing temperature drops, respectively, plotted against operating temperature and heat flux for a number of vapor chamber working fluids.

Another important parameter that can be used to evaluate vapor chamber working fluids is the 0-g capillary pumping length. This parameter gives the maximum length of the condensing portion of the vapor chamber. Beyond this length, the friction pressure drop in the wick is too great for capillary forces to overcome. Thus, the working fluid cannot recirculate.

This applies only at zero gravity conditions. Capillary pumping length in 0-g was obtained by equating the capillary pumping head with the head required to overcome friction. Laminar flow was assumed in the model. To calculate capillary pumping head, the effective radius

[2] McAdams, W.H., "Heat Transmission," McGraw-Hill, 1954

[3] Cichelli, M.T., and Bonilla, C.F., Trans. AIChE, Vol 41, pp 755, 1945

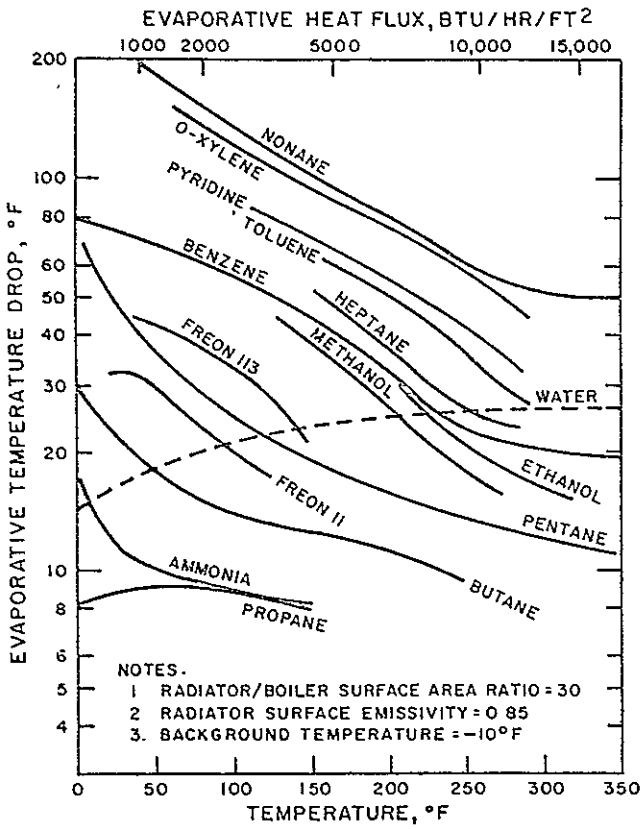

Figure 3. Evaporative Temperature Drop

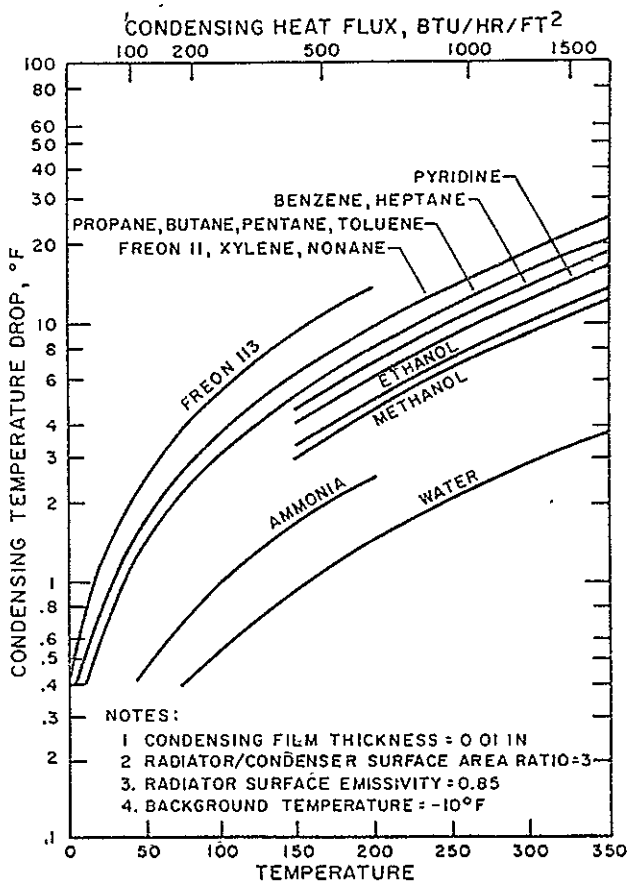

Figure 4. Condensing Temperature Drop

of curvature was assumed to be 0.003 inch. Under gravity conditions, the capillary forces will also have to pump against the liquid head in the vapor chamber. The 1-g capillary pumping height is a measure of the maximum head that a working fluid can supply. Figures 5 and 6 show the variation of the 0-g capillary pumping length and the 1-g capillary pumping height, respectively, as a function of operating temperature for various working fluids. For Figure 6, the assumption is made that the friction loss is equal to one-half the capillary pumping head. The effective radius of curvature was again assumed to be 0.003 inch.

To keep radiator area at a minimum, the evaporative and condensing temperature drop must be small. To insure adequate circulation of the working fluid, the 0-g capillary pumping length must be large. Since the radiator has to be tested under 1-g conditions, it is also important that the 1-g capillary pumping height be large. A comparison of Figures 3 through 6 shows that ammonia and the Freons offer the best promise as working fluids at temperatures below about 150°F. At operating temperatures above 150°F, water, the alchohols, pentane and benzene offer the best promise.

Before selecting vapor chamber working fluids to be used in the radiator designs, the compatibility of the fluids with the 6061-T6 aluminum alloy was determined. These compatibility tests were performed in capsules about 0.5 inch diameter by 24 inches long. A single layer of 120-mesh aluminum screen was inserted along the entire length of the capsules. The bottom of the capsule was heated in an oil bath at temperatures up to about 300°F, depending on the fluid under test. The capsule was cooled at the top by flowing ambient air. Each capsule was instrumented with thermocouples such that the temperature along the top 4 inches of the condensing portion could be monitored. Differences in temperatures along this portion of the capsule indicated the formation of noncondensable gas. After test the capsules were sectioned for evidence of corrosion damage to the aluminum alloy or chemical change to the working fluid.

The results of the compatibility tests are shown in Figure 7. Based on the results of the compatibility tests and the data given in Figures 3 through 6, the following vapor chamber working fluid combination was selected for the vapor chamber radiator design:

Ammonia at temperatures up to 150°F

Pentane at temperatures above 150°F

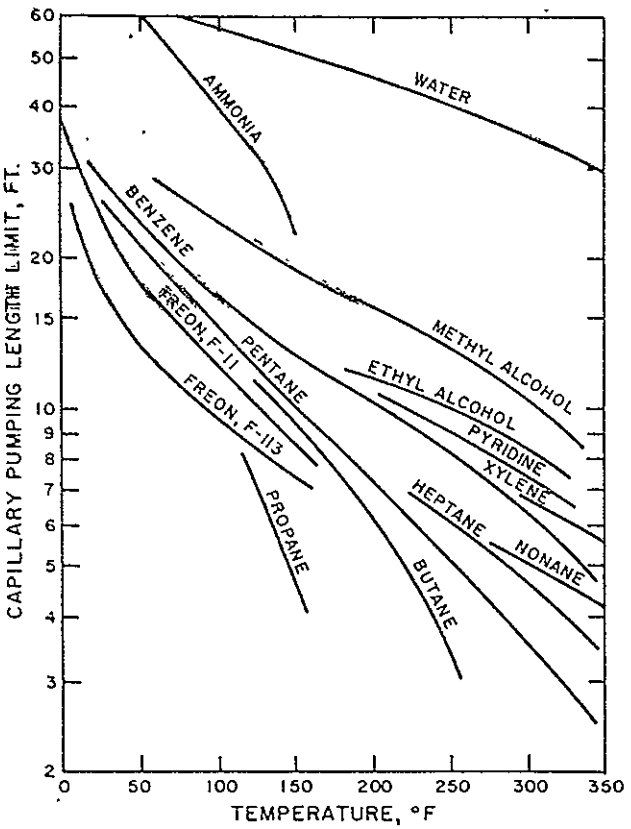

Figure 5. Zero-G Capillary Pumping Limit

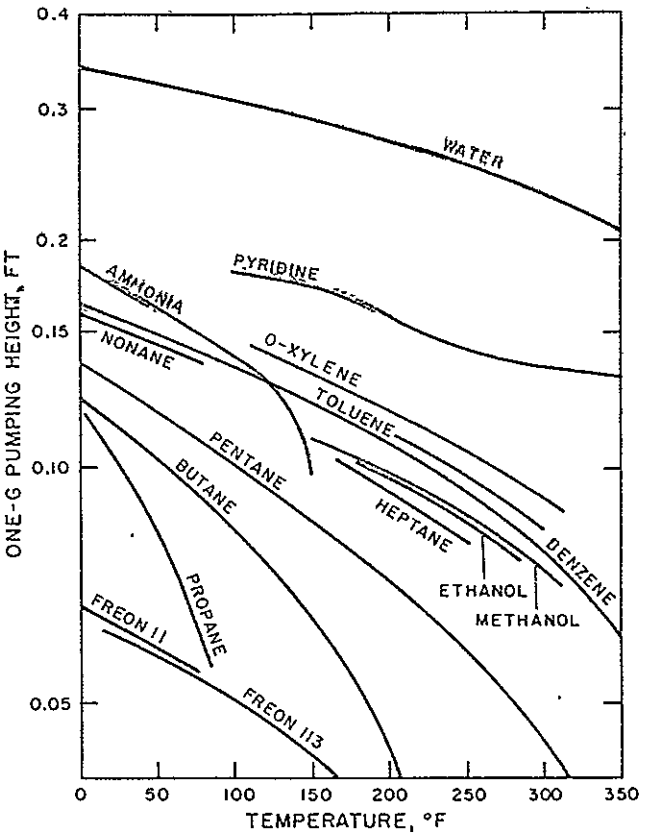

Figure 6. One-G Capillary Pumping Height

CAPSULE IDENTIFICATION	FLUID	TEST TEMP., °F	TEST HOURS	TEST RESULTS
C-1	METHYL ALCOHOL	NOT TESTED	-	GAS GENERATED DURING FILL
C-2	N-PENTANE	316	570	NO GAS, NO CORROSION, SLIGHT FLUID DISCOLORATION
C-3	BENZENE	316	570	GOOD
D-1	AMMONIA	159	500	GOOD
D-2	FREON 11	156	500	GOOD
D-3	FREON 113	155	500	GOOD
D-4	TOLUENE	323	600	GOOD
D-5	N-HEPTANE	321	600	GOOD
D-6	PYRIDINE	318	550	NO GAS, BUT DEPOSITS AND FLUID DISCOLORATION OCCURRED
D-7	CP-34	319	550	SLIGHT GAS AND FLUID DISCOLORATION
D-8	FREON 113	224	500	GOOD
D-9	FREON 11	222	500	GOOD
D-11	N-BUTANE	150	500	GOOD

Figure 7. Compatibility Test Results

Since benzene indicated more capillary pumping capability than pentane, some design analyses were also made using benzene as the high temperature vapor chamber working fluid.

METHOD OF ANALYSIS

Formulation of the radiator design involved consideration of many factors. These included (1) shape of radiator, (2) size and number of panels, (3) size and number of coolant headers, (4) whether coolant headers were lengthwise or cross wise of panels, and (5) meteoroid protection approach. A cylindrical shape radiator was the preferred approach for satisfying the powerplant requirements. The circumference of both primary and secondary radiators was divided into six panels. To minimize circumferential temperature gradients, the coolant flow as lengthwise of the panels.

Design of the coolant ducts for both the vapor chamber and conducting fin radiators posed a difficult problem. Analysis showed that these ducts could not be designed to flow turbulent without encountering very high pressure drops (more than 1000 psi). Since heat transfer in laminar flow is poor, the temperature drop between the coolant and the duct wall was large. A solution to this problem was found. The heat transfer between the coolant and the duct wall was improved by using very small hydraulic passages, on the order of 0.010 inch. These small passages were produced by placing many thin, closely spaced fins in a rectangular coolant duct. Coolant flow in the passages was laminar (Reynolds number of about 50), and the coolant to duct wall temperature drop was about 10°F. The convective laminar heat transfer coefficient for the coolant was calculated using the Sieder-Tate equation[2].

The calculation of the other temperature drops between the coolant and the radiating surface were done as follows. For the vapor chamber, the evaporative and condensing temperature drops were calculated using the assumptions described earlier. Temperature drops across the duct armor, vapor chamber walls and bumper fins were comparatively small. The thicknesses of the armor, walls, and bumper fins were determined from the meteoroid damage criteria. Protection against meteoroid damage was provided by either bumpers or armor whichever was lighter for each situation.

Both the vapor chamber and conduction fin radiators were studied for overall meteoroid survival probabilities ranging from 0.990 to 0.999. The overall survival probability of the radiator was equal to the multiple of the individual survival probabilities of each of the radiator components. Failure probabilities were weighted as follows: four primary radiator failures to one secondary radiator failure, and nine duct system failures to one vapor chamber system failure. (A duct system failure is defined as failure of both coolant circuits, one circuit being redundant. A vapor chamber system failure is a failure of more than 15 percent of the vapor chambers, 15 percent being the design redundancy.)

The design loads for the radiators are determined by the loads that occur during launch. The two conditions of interest during the launch trajectory are the times at which maximum lateral and maximum axial accelerations occur. The load factors for these conditions are a function of payload weight. For a payload of approximately 6000 pounds (powerplant including radiator), the load factors of the Atlas-Centaur launch vehicle using the Orbiting Astronautical Observatory (OAO) are stated[4]:

	Axial Load Factor	Lateral Load Factor
Maximum axial acceleration condition	6.2	0.3
Maximum lateral acceleration condition	2.3	1.56

For design purposes, the launch loads are most conviently expressed in terms of equivalent axial load[5].

$$P_{eq} = P_{ax} + 2M/R$$

where

P_{eq} = equivalent axial load

P_{ax} = axial load

M = bending moment

R = radius of radiator

The approximate radiator areas and corresponding design loads used in the structural analysis were:

	Area	Shear Load	Equivalent Axial Load
Conducting fin radiator	475 ft^2	10900 lb	94000 lb
Vapor chamber fin radiator	508 ft^2	10900 lb	99000 lb

Both the vapor chamber and conducting fin radiators were optimized by computer analyses. Trade-off factors were used to convert coolant pressure drops and radiator area into equivalent power system weights. These equivalent weights were added to the actual radiator weight yielding an effective radiator system weight. The radiator design was then varied until a minimum effective radiator system weight was obtained. By using trade-off

[4] "Centaur Payload User's Manual," NASA CR-72190, August 1966

[5] Cockfield, R.D., "Definition of Spacecraft and Radiator Interrelations for Nuclear Rankine Systems," NASA CR-72245, January 26, 1967

factors, such as coolant pumping power penalty in lb/kW to trade-off for pressure drop and area penalty in lb/ft^2 to trade-off for large area, the sensitivity of the radiator design to pressure drop and area was examined. Pressure drop was found to have little influence on radiator design. As the coolant pumping power penalty was varied from 0 to 4000 lbs/kW, the effective radiator system weight varied about 10 percent. This small change in radiator system weight produced a negligible change in the radiator design. Radiator area penalty, however, was a sensitive trade-off variable. In the radiator designs that follow, the area penalty was varied from 0 to 5 lb/ft^2. Over this range, the effective radiator system weight varied about 500 percent. For this reason, the radiator optimized at smaller areas but at larger weights.

In the comparison of vapor chamber and conducting fin radiators, only the primary radiator for each was considered. The primary radiator was about 75 percent of the total weight and area in each case. A preliminary analysis showed that the comparison of primary radiators gave the same results as a comparison of total radiators. This conclusion also held when the same radiator was compared at different survival probabilities.

VAPOR CHAMBER RADIATOR DESIGN

Both primary and secondary radiators are combined into a single hexagonal shaped assembly, as shown in Figure 8, measuring 115 inches across and 215 inches long. Each side of the hexagon contains one primary radiator panel and one secondary panel. The end transverse sections are mounting flanges to integrate with the launch booster on one end, and the supported load on the other end.

A primary radiator coolant duct is located at the center of each radiator panel. This rectangular duct, approximately 1.0 inch high by 1.5 inches wide, contains two sets of coolant flow passages, one of which is redundant (see inset of Figure 8). Each set of duct passages contains 55 plate fins, 0.005 inch thick. Each coolant flow passage is rectangular in cross-section, 0.013 inch by 0.150 inch. Between the two sets of coolant passages are located the evaporator sections of the vapor chambers. The vapor chamber will reject heat from either coolant circuit. Square holes between the evaporator sections eliminate the weight of material not needed for heat transfer. The duct is protected by 0.200 inch armor thickness.

Manifolding of the coolant lines leading to the ducts is accomplished by use of plenums and tube sheets located at the powerplant assembly. Each duct contains two 0.5 inch tube connections at each end, one for each of the two coolant circuits.

Vapor chambers extend perpendicularly from the sides of the ducts. Fill tubes for the vapor chamber extend from one side of the duct while the vapor chamber extends

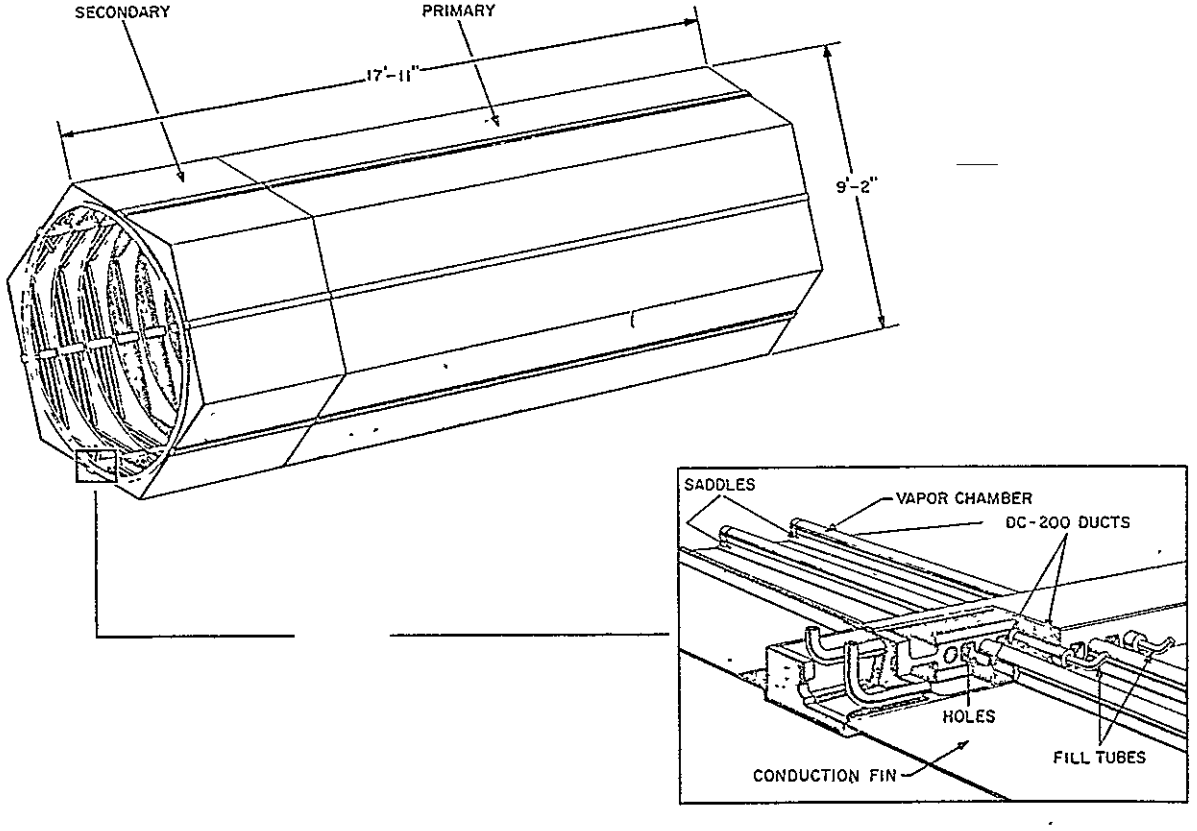

Figure 8. Vapor Chamber Radiator Conceptual View

from the other side. Each vapor chamber is 26.2 inches long, 0.31 inch outside diameter, and has a 0.015 inch wall. Within the vapor chamber, 120 mesh aluminum wire cloth is used for the wick material. A total of 1969 vapor chambers are required; 1537 for the primary radiator (340 pentane, 1197 ammonia), and 432 for the secondary radiator (ammonia). Of these, 15 percent can be lost by meteoroid puncture or other causes and still satisfy the thermal heat load.

The outer skin of the radiator panel is a 0.021 inch thick conduction fin, upon which the vapor chambers are mounted by use of a saddle shaped support. Vapor chambers are spaced 1.31 and 1.57 inches apart on centers on the primary and secondary radiator panels, respectively. The conduction fin serves as a meteoroid bumper to protect the vapor chambers. This fin is sufficiently thick that if one vapor chamber fails, the area and temperature loss is so negligible the radiator can still reject its design head load.

Support for vertical acceleration of the radiator and 5000-pound load is provided by the six coolant ducts. Shear loads due to transverse moments are carried by the conduction fin sheet. Although the vapor chambers provide panel stiffening, a total of 19 stiffening bulkheads, or rings, are required to sufficiently stiffen the overall radiator assembly. In addition, mounting bulkheads are located at the bottom and top of both primary and secondary radiators. All of these bulkheads are Z shaped sections. The radiator panels are connected at their edges.

Figure 9 tabulates the weights and areas of the vapor chamber primary and secondary radiators at survival probabilities of 0.990 and 0.999. For all practical purposes, the weight and area of the vapor chamber radiator is unchanged over the range of survival probabilities studied. The radiator design shown in Figure 8 and the weights and areas tabulated in Figure 9 were generated using a coolant pumping power-penalty for pressure drop trade-off of 4000 lb/kW and a penalty for area trade-off of 3 lb/ft^2. These designs were selected as the design point radiators.

Figure 10 shows the vapor chamber primary radiator weight as a function of its area. This figure was generated by varying the penalty for area trade-off from 0 to 5 lb/ft^2. An area trade-off of zero gives the minimum weight radiator. The minimum or ideal area, shown by the vertical dashed line, occurs when there is no temperature drop between the coolant and the radiating surface. The weight of an ideal area radiator would approach infinity. At a survival probability of 0.999, the minimum weight radiator is 45 percent larger and the design point radiator is 36 percent larger than ideal. Changing the survival probability from 0.999 to 0.990 caused a negligible decrease in radiator area and weight. Again, the significant characteristic of the vapor chamber radiator is its insensitivity to meteoroid protection requirements.

SURVIVAL PROBABILITY	0.990	0.999
WEIGHT TABULATION		
PRIMARY RADIATOR		
DC-200 DUCTS	112	117
VAPOR CHAMBERS	131	133
CONDUCTION FINS	113	113
PANEL SPLICE JOINTS	16	16
STIFFENING RINGS	78	78
TOTAL	450	457
SECONDARY RADIATOR		
DC-200 DUCTS	33	35
VAPOR CHAMBERS	39	40
CONDUCTION FINS	34	34
PANEL SPLICE JOINTS	5	5
STIFFENING RINGS	36	36
TOTAL	147	150
TOTAL RADIATOR WEIGHT	597	607
AREA TABULATION		
PRIMARY RADIATOR	377	379
SECONDARY RADIATOR	127	127
TOTAL RADIATOR AREA	504	506

Figure 9. Vapor Chamber Radiator Weights and Areas

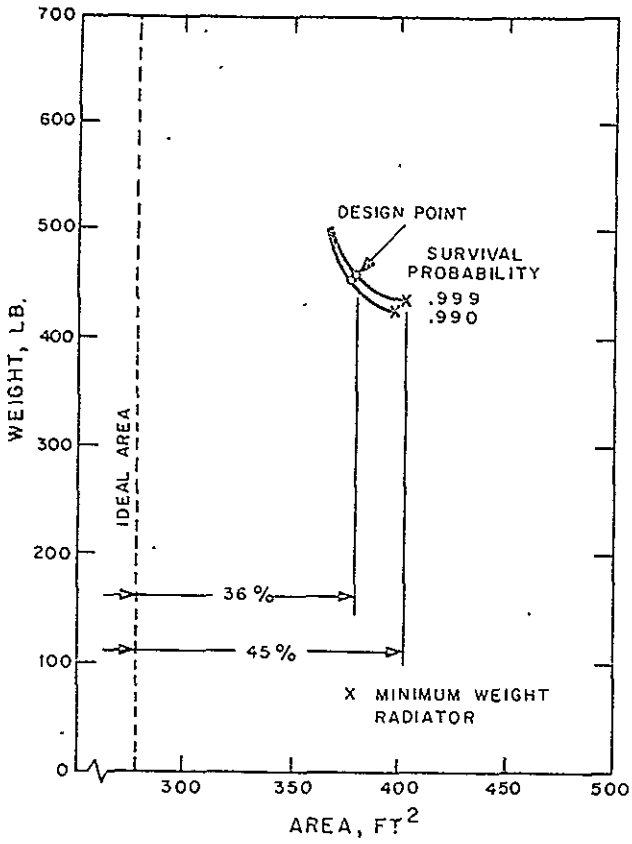

Figure 10. Vapor Chamber Primary Radiator Performance Characteristics

CONDUCTION FIN RADIATOR DESIGN

In the conduction fin radiator, both primary and secondary radiators are also combined into a single assembly. This assembly, shown in Figure 11, is cylindrical in shape, measuring 110 inches in diameter and 198 inches long. Each 60-degree segment contains one primary radiator panel and one secondary radiator panel.

The coolant (DC-200) flows through rectangular ducts, 0.3 by 0.5 inch outside dimensions. Each duct contains 10 rectangular fluids passages, each 0.010 by 0.200 inch in cross-section and separated by 0.005 inch plate fins. Two sets of seven ducts each are provided per panel, one set for each of two coolant circuits. Meteoroid protection is provided by a layer of 0.084 and 0.067 inch of armor for the primary and secondary radiators, respectively.

Each of the two sets of seven coolant ducts are connected to a 0.5 inch inside diameter manifold on each end of a panel. Plumbing lines from these manifolds are routed to the other powerplant components in a manner identical to that of the coolant ducts for the vapor chamber radiator.

The outer skin of the radiator panel comprises a conduction fin of 0.063 and 0.058 inch in thickness for the primary and secondary radiators, respectively. Coolant ducts for primary and secondary radiators are 4.0 and 4.7 inches on centers; fin efficiencies are 92.0 and 93.5 percent, respectively.

The conduction fin radiator is structurally better than the vapor chamber fin radiator. However, the conduction fin radiator also requires additional interface and stiffening rings. Splice joints join the radiator panels at their edges.

Figure 12 tabulates the weights and areas of the conduction fin primary and secondary radiators at survival probabilities of 0.990 and 0.999. For the conduction fin, survival probability significantly affects the radiator weight. The design point conduction fin radiators were calculated using the same pressure drop and area trade-offs used for the vapor chamber radiator.

Figure 13 shows the conduction fin primary radiator weight as a function of its area. At a survival probability of 0.999, the minimum weight radiator is 56 percent larger and the design point radiator 28 percent larger than ideal. Changing the survival probability from 0.999 to 0.990 reduces the weight at constant radiator area by 25 percent.

COMPARISON OF VAPOR CHAMBER TO CONDUCTION FIN

The vapor chamber primary radiator is compared to the conduction fin primary radiator in Figure 14 for 0.999 and 0.99 survival probability. At the selected design points for 0.999 survival probability, the conduction fin radiator is 22 percent heavier and 7 percent smaller than the vapor chamber fin radiator. At minimum weight and 0.999 survival probability, the conduction fin radiator is 14 percent heavier and 8 percent larger than the vapor chamber fin radiator. At an area of 379 ft^2, which is the design point area, the conduction fin radiator is 12 percent heavier. Thus, at a survival probability of 0.999, the vapor chamber fin radiator is superior in weight and area when compared to the conduction fin radiator. However, at 0.990 survival probability, the comparison reverses. At 379 ft^2 radiator area, the conduction fin radiator is lighter by 17 percent. Interpolating between survival probabilities at 379 ft^2, the weights of vapor chamber and conduction fin radiators are identical at a 0.998 survival probability. Above this probability, the vapor chamber radiator is advantageous, while below this, the conduction fin radiator is advantageous.

As was stated earlier, the Cichelli and Bonilla correlation was used to calculate the evaporative temperature drop in the vapor chambers. If experimental data result in different temperature drops, the comparison between the vapor chamber and conduction fin radiators will change. Temperature drops larger than predicted from Cichelli and Bonilla would increase the area and weight of the vapor chamber radiator, and vice-versa.

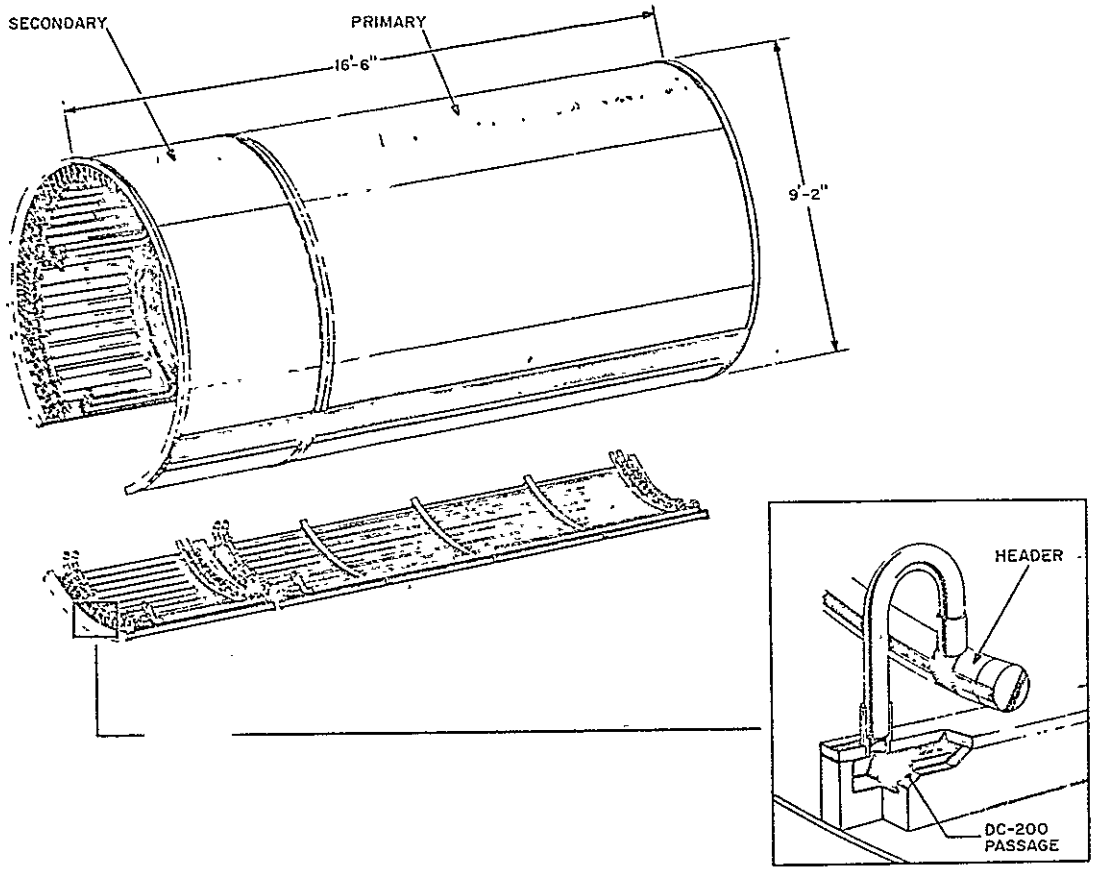

Figure 11. Conduction Fin Radiator Conceptual View

SURVIVAL PROBABILITY	0.990	0.999
WEIGHT TABULATION		
PRIMARY RADIATOR		
DC-200 DUCTS	169	198
CONDUCTION FINS	229	311
HEADERS	6	6
PANEL SPLICE JOINTS	15	15
STIFFENING RINGS	30	30
TOTAL	449	560
SECONDARY RADIATOR		
DC-200 DUCTS	36	42
CONDUCTION FINS	72	98
HEADERS	5	5
PANEL SPLICE JOINTS	5	5
STIFFENING RINGS	10	10
TOTAL	128	160
TOTAL RADIATOR WEIGHT	577	720
AREA TABULATION		
PRIMARY RADIATOR	347	355
SECONDARY RADIATOR	119	122
TOTAL RADIATOR AREA	466	477

Figure 12. Conduction Fin Radiator Weights and Areas

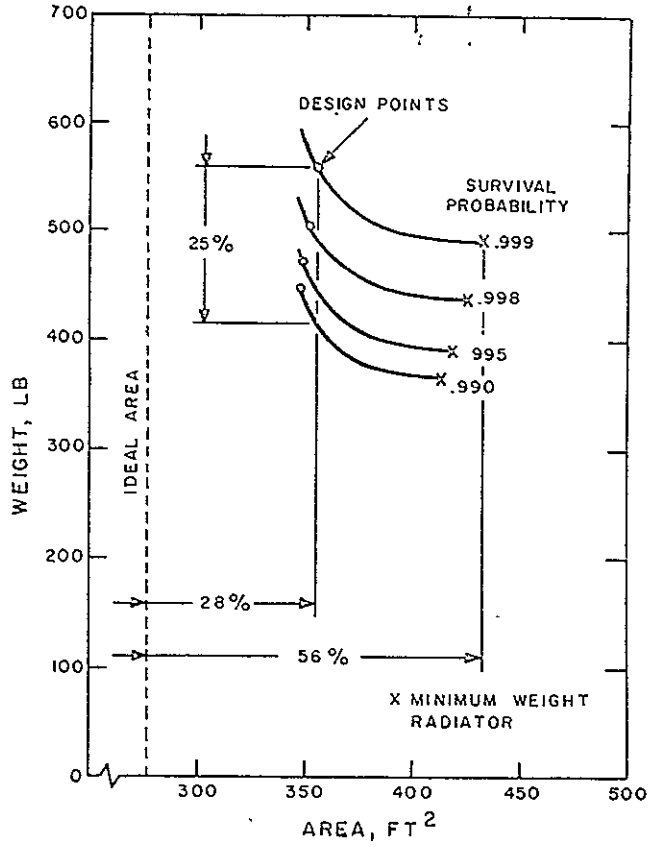

Figure 13. Conduction Fin Primary Radiator Performance Characteristics

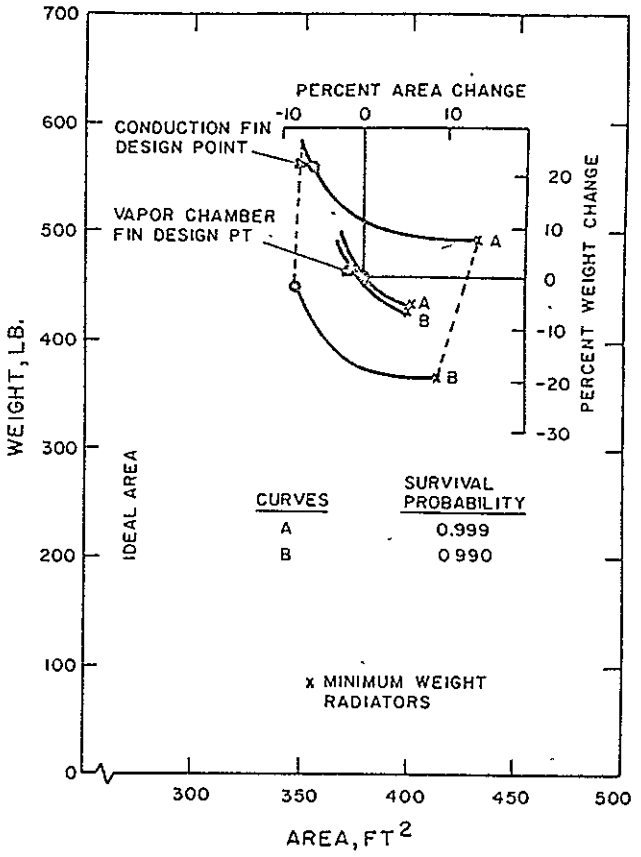

Figure 14. Comparison of Vapor Chamber Fin to Conduction Fin Primary Radiators

The condensing temperature drop in the vapor chambers was calculated assuming conduction through a 0.010 inch film of the working fluid. Experimental data will support or refute this assumption. In addition, the organic working fluids have poor 1-g capillary pumping heights when compared to water and ammonia. A remaining unknown will be whether vapor chamber performance data at 1-g can be used to predict 0-g operation in space.

COMPARISON OF VAPOR CHAMBER WORKING FLUIDS

Although pentane and ammonia were selected for the vapor chamber radiator reference design, other fluids are also of interest. Radiator weights versus area are compared in Figure 15 for five combinations of working fluids for a survival probability of 0.999. Curve A shows the pentane/ammonia combination as was shown in Figure 10. Benzene, desirable because of its good wicking characteristics, is paired with ammonia in Curve B; it shows a 14 percent increase over pentane in radiator weight at 379 ft^2. Butane/ammonia, Curve C, is 2 percent lighter than pentane/ammonia. Water, one of the best fluids, is paired with ammonia in Curve D. However, water alone is inferior to water/ammonia, as shown in Curve E.

In conclusion, water/ammonia is the best selection to satisfy the specified requirements, but butane, pentane or benzene can replace water with only a small penalty. However, water was found to be incompatible with aluminum and can be used only if the aluminum is lined with a compatible material such as copper, nickel, gold or silver. The additional weight for this liner has been estimated as about 2 percent of the total radiator weight. This additional weight is not included in Curves D and E of Figure 15.

CONCLUSIONS

A vapor chamber fin radiator concept has been evaluated and compared with a conduction fin radiator for the Brayton cycle space powerplant specified in Figure 1. The following conclusions have been reached:

1) Of the fluids tested, ammonia is the best working fluid for vapor chambers operating at temperatures below 150°F.

2) At operating temperatures above 150°F, water is the best working fluid on the basis of performance calculations. However, since water

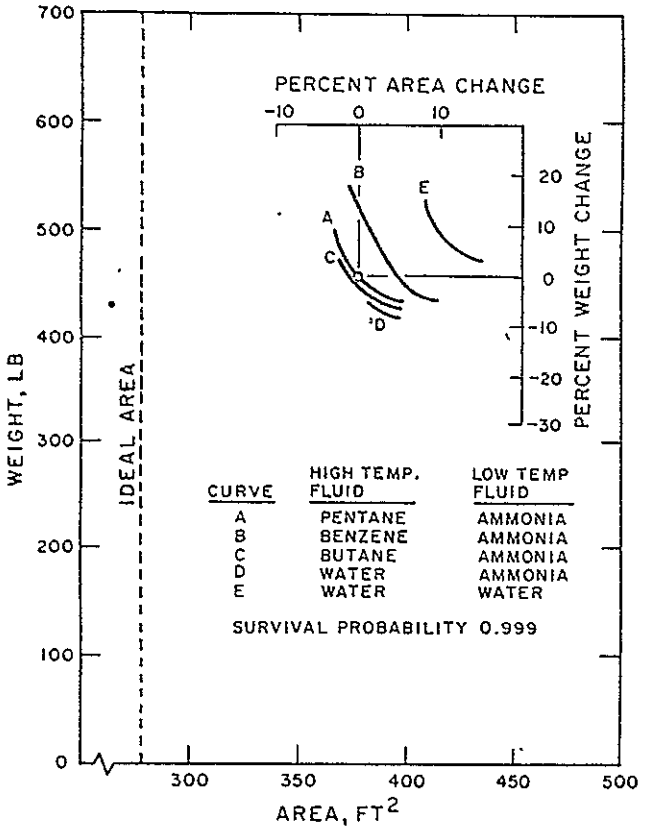

Figure 15. Comparison of Vapor Chamber Working Fluids

is incompatible with aluminum and a liner was not considered, pentane was selected as the working fluid in this temperature range.

3) The vapor chamber radiator is insensitive to meteoroid survival probability when compared to the conducting fin radiator.

4) The specific weight for both radiator types ranges between 1.0 and 1.5 lbs/ft^2.

5) Both radiators seem to be about equal in weight and area at a survival probability of 0.998. At higher probabilities, the vapor chamber radiator seems to be lighter and smaller, while at lower probabilities the conduction fin radiator is lighter and smaller. However, the differences in weight and area are less than 20 percent over the range of probabilities from 0.990 to 0.999.

ACKNOWLEDGEMENTS

The authors wish to thank Mr. Arthur Schnacke for the formulation of the basic vapor chamber concept and analysis; Dr. Ted Lyon for the performance of the compatibility experiments; Mr. Robert Cockfield for the radiator structural design and analyses; and Mr. Robert Killen for the thermodynamic, fluid and system optimization analyses.